Volume 336, number 3, 397–402 FEBS 13449 December 1993

Structural study of rat thyroid transcription factor 1 homeodomain (TTF-1 HD) by nuclear magnetic resonance

Paolo Viglino[a], Federico Fogolari[a], Silvestro Formisano[a], Nadia Bortolotti[b], Giuseppe Damante[a], Roberto Di Lauro[a], Gennaro Esposito[a,*]

[a]*Dipartimento di Scienze e Tecnologie Biomediche, Università di Udine, Via Gervasutta, 48, 33100 Udine, Italy*
[b]*Laboratorio Analisi USSL 7, Via Gervasutta, 48, 33100 Udine, Italy*

Received 21 September 1993; revised version received 11 November 1993

The 500 MHz ^{1}H NMR spectrum of a 68-residue peptide, encompassing the rat thyroid transcription factor 1 homeodomain (TTF-1 HD), was fully assigned using standard 2D NMR methodology. The secondary structure elements and their spatial organization were determined and led to a structure very similar to that previously described for other homeodomains and expected also for TTF-1 HD from homology modeling predictions. The three-dimensional arrangement of the three helix fragments of TTF-1 HD preserves the helix–turn–helix motif commonly occurring in many classes of DNA-binding proteins.

Thyroid transcription factor 1 (TTF-1); Homeodomain; Protein NMR

1. INTRODUCTION

Thyroid transcription factor 1 (TTF-1) is a homeodomain-containing protein responsible for transcriptional activation of genes expressed in follicular thyroid cells [1,2]. Homeodomains (HDs) are DNA-binding protein domains, approximately 60 residues long, that are encoded by highly conserved DNA stretches, the homeoboxes, occurring in several genes involved in transcriptional regulation [3,4].

One of the basic features of proteins encoded by homeobox-containing genes is the sequence-specific DNA recognition by homeodomains.

Since different homeodomains can preferentially recognize distinct DNA sequences, the elucidation of the mechanism responsible for differential DNA recognition is an important step towards the understanding of their role.

To date only three HD–DNA complexes have been structurally characterized by NMR or X-ray cristallography, i.e. the complex of Antennapedia (*Antp*) [5], engrailed (*en*) [6] and MAT α2 [7], while the solution structure of isolated HD molecules has been published for *Antp* [8,9] and MAT α2 [10].

The secondary structure of the *oct-3* POU HD, obtained by NMR has also been reported preliminarly [11]. For POU homeodomains, however, the actual DNA complex entails the simultaneous association of an additional domain, the POU specific domain [11], contrary to the other HD classes that, in addition, keep binding their DNA targets also when excised from the entire protein.

All the known structures show the predicted helix–turn–helix (HTH) DNA-binding motif and a similar arrangement of DNA contacts [4,12], but the whole complex geometry looks rather different from the one observed with prokaryotic proteins possessing the same HTH motif [12].

Even though a common framework emerges for the binding of several homeodomains to DNA, structural studies of particular complexes appear crucial to address the issue of modulation of DNA-binding specificity.

In this respect, the rat TTF-1 HD, which has a sequence rather divergent from the general HD consensus [4], raises a certain interest because the first 7 residues out of 10 of helix III, i.e. most of the putative recognition helix [4,12], are identical to the consensus sequence, and yet the molecule exhibits preferential binding to a DNA sequence devoid of the TAAT core stretch [2], most commonly recognized by homeodomains [13].

Previous mutagenic investigations had shown that the DNA-binding specificity of TTF-1 must involve also regions outside the recognition helix and that a progressive DNA-binding specificity switching is obtained when swapping single regions of the molecule with the corresponding portions of *Antp* HD [14]. These findings were partially rationalized on structural grounds by a homology modeling study of the DNA-bound domain [15].

In this communication a first account is presented of the structural characterization by high-resolution NMR

*Corresponding author. Fax: (39)(432) 600 828. *Present address:* Section de Chimie, Université de Lausanne, Rue de la Barre 2, CH 1005 Lausanne, Switzerland. Fax: (41) (21) 316 3728.

spectroscopy of a 68-residue peptide encompassing the rat TTF-1 HD. The complete assignment of the 500 MHz ^{1}H NMR spectrum was achieved and, from subsequent interpretation of the data, the emerging structural picture largely confirmed the results obtained by preliminar homology modeling [15].

2. MATERIALS AND METHODS

The TTF-1 HD polypeptide (68 residues corresponding to fragment 160–226 of the entire rat TTF-1 molecule [2], plus a methionyl residue appended at the N-terminus, MW 8811 Da) was obtained from overexpression in *E. coli*, strain BL21, of the corresponding DNA sequence cloned into vector pT7.7 [16].

The construction of this vector, the bacterial growth conditions and the extraction protocol of the polypeptide material were reported elsewhere [2]. The purification of the crude product was achieved by ion-exchange chromatography, adopting the same procedure as described for *Antp* HD [17]. The overall final yield was 0.5–1 mg pure protein per liter of culture.

NMR samples were prepared by dissolving the lyophilized powder in H_2O/D_2O 90/10 or pure D_2O (Sigma), always containing 0.15% w/v NaN_3, and adjusting the pH to 4.1 (meter reading) by micro-additions of HCl or DCl. The protein concentration was about 5.5 mM.

^{1}H NMR spectra were obtained at 287 and 289 K on a Bruker AM500 spectrometer. Two-dimensional TOCSY [18], DQF COSY [19] and NOESY [20] were collected in the pure phase mode, employing the TPPI procedure [21] for F1 quadrature. Mixing times (t_m) were selected in the range 25–49 ms and 80–150 ms for TOCSY and NOESY, respectively.

The experimental matrix dimensions were typically 2–3K points in F2 and 500–700 points in F1 for a spectral window of 7462.7 Hz in both dimensions. All data were processed on Silicon Graphics computers using the software package FELIX (Hare Research Inc.). Shifted sine-bell squared resolution enhancement and zero filling were applied prior to 2D FT, to end up with 2K × 2K real point matrices. Chemical shifts were referred to the resonance of dioxane (3.767 ppm) added as an internal standard to the samples. Structure modeling and analysis were performed using the Biosym Technologies software INSIGHT II [22] and the programs WHATIF [23] and DIANA [24]. Based on quantitation of the dipolar and scalar connectivity information 600 meaningful upper and lower distance bounds and 27 χ^1 angle restraints were imposed. The standard minimization protocol of the program DIANA was employed [24].

3. RESULTS AND DISCUSSION

Preliminary spectra of TTF-1 HD acquired at 298 K proved poorly informative because of thermal lability of the isolated molecule structure, as confirmed also by independent CD studies (S. Formisano et al., in preparation).

The amount and quality of information considerably improved on lowering the temperature by some ten degrees. The results presented here are from data obtained at 287 and 289 K.

Determination of the three-dimensional structure of a protein from NMR data requires the backbone and side chain proton resonances to be assigned.

The procedure we followed to this aim employed both of the two most commonly applied strategies for protein NMR analysis, namely the sequential assignment approach [25] and the main chain directed approach [26].

Depending on whether the particular group of considered resonances exhibited favourable spectral

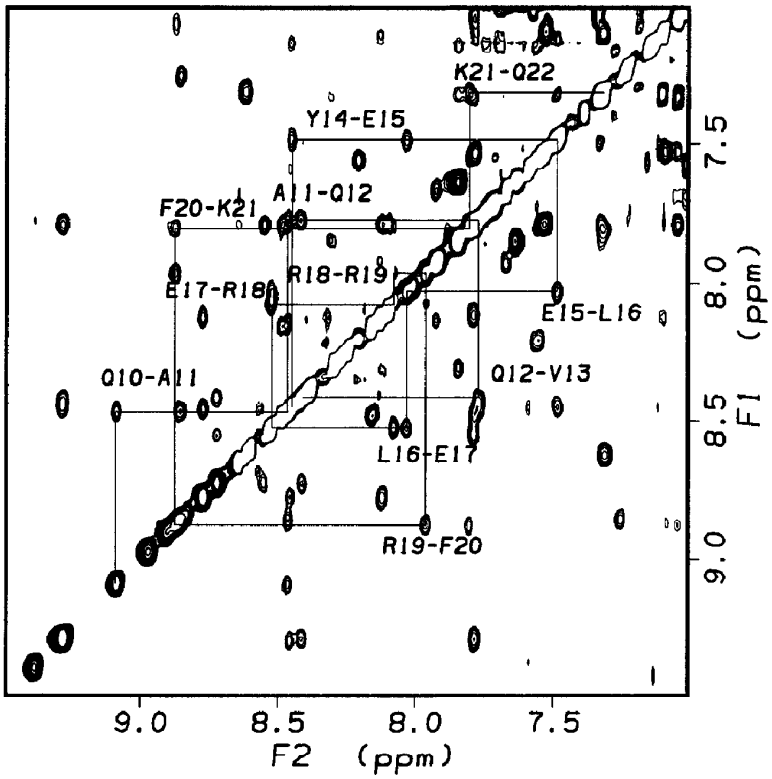

Fig. 1. Amide region of the 500 MHz ^{1}H NOESY spectrum of TTF-1 HD in H_2O/D_2O (90/10) at 289 K and mixing time 80 ms. NH-NH connectivities in the first helix (spanning residues 10–22) are labeled using the amino acid single letter code.

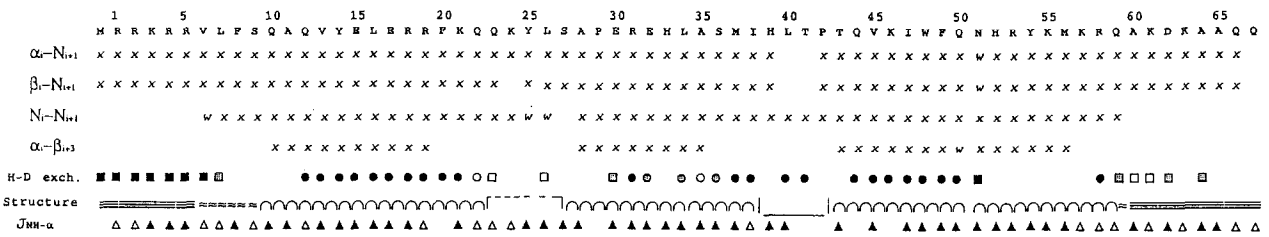

Fig. 2. Synopsis of some diagnostic NOE connectivities (sequential and short range) observed for TTF-1 HD. Only qualitative information is displayed, except for some weak connectivities (marked with *w*). Amide H–D exchange data from TOCSY spectra are reported using circles or boxes for the resonances exhibiting, respectively, limited or extensive average intensity decrease after 6 h isotope exchange. Filled, shadowed and empty symbols indicate the subsequent intensity loss extent after 11.5 h exchange (filled, minor loss; shadowed, substantial loss; empty, total loss). $J_{NH-\alpha}$ estimates are also provided, when available from high resolution DQF COSY data. Filled triangles indicate $J_{NH-\alpha} \leq 6$ Hz, empty triangles $J_{NH-\alpha} > 6$ Hz. The secondary structure symbols correspond to: α-helix (curly line); fraying edges (weavy lines); disordered regions (straight lines); loop (dashed line); tight turn (solid line).

spread, the former or the latter were alternatively chosen. Thus, for instance, the sequence specific identification of virtually every aromatic and valine spin systems, as well as that of most leucines, was attained by sequential assignment, while for the amino- and carboxy-terminal residues only the main chain directed approach was really viable.

Fig. 1 illustrates amide protons sequential connectivities in the NOESY spectrum among residues 10–22 spanning the first helix of TTF-1 HD.

The achievement of complete sequence-specific assignment of a protein spectrum is intimately related to the determination of the secondary structure of the molecule [25,26], a necessary piece of information to further establish spatial relationships among different structural elements and, ultimately, define the overall three-dimensional arrangement.

Fig. 2 provides the symbolic overview of the secondary organization of TTF-1 HD in aqueous solution, as inferred from analysis of approximately 1200 NOESY connectivities. $J_{NH-\alpha}$ coupling constant estimates and isotope exchange data are also displayed. The latter were obtained by analysis of two consecutively acquired TOCSY spectra (t_m=15.6 ms) on a protein sample freshly dissolved in D_2O. The residual NH-αCH cross-peak intensities reflect the mean isotope exchange occurred at 6 and 11.5 h from sample preparation.

The complete list of chemical shifts is reported in Table I.

Only the presence of diagnostic connectivities is indicated in Fig. 2, the report of the corresponding quantitative information being deferred to a forthcoming paper. The general features of the secondary structure of TTF-1 HD, however, are already evident from the picture of Fig. 2.

Three α-helix segments can be recognized, which span through fragments 10–22, 28–38 and 43–59. The third helix appears flexible at the C-terminal portion, namely between residues 52 and 59 (referred to as helix IV for *Antp* HD [8,9]), as deduced from H–D exchange data. The series of slow-exchanging amide protons, in fact, breaks down at His-52.

Hydrogen bonds between the carbonyl oxygen of residue *i* and the amide hydrogen of residue (*i* + 4) of regular α-helices are usually manifested by slow isotope exchange of the NH's.

Some departure from this behaviour observed in Fig. 2 can be readily rationalized, for instance, for most of the amides at the helix N-termini, where N-capping effects [27] also compensate for the expectedly missing H-bond capability, as well as for His-33 NH, where the correct geometry required for hydrogen-bonding is conceivably distorted by the proline residue four positions upstream.

Instead, the fast amide exchange observed in region 52–58, in the presence of short and medium range helical connectivities and $J_{NH-\alpha} \leq 6$ Hz, should be ascribed to inherent flexibility of the local structure.

A similar conclusion has been reported also for the other comparable studies of HD solution structure performed to date, i.e. *Antp* [8,9] and MAT α2 [10]. For *oct-3* POU HD, fraying edge effects could be invoked because a sequence truncated at residue 60 was investigated [11].

In TTF-1 HD, the mobility of the helix III terminal tract is, in addition, independently confirmed by the increase of the corresponding cross-peak intensities in the fingerprint region of DQF COSY spectra.

Antiphase cross-peak cancellation, in fact, depends on the active coupling/linewidth ratio [23,8]; therefore a relative intensity increase is expected as linewidth decreases, which for NH-αCH connectivities mostly reflects a local increase of backbone mobility.

According to the last criterion and to isotope exchange data (Fig. 2), also helix II exhibits some segmental flexibility, a feature reported for MAT α2 HD [10] but not for *Antp* [8,9].

Like in all homeodomains, however, the three helices of TTF-1 HD are joined by a loop (region 23–27) and a tight turn (region 39–42). This latter corresponds to

Table I

Proton chemical shifts, referenced to internal dioxane (3.767 ppm). For methylene groups the presence of a single chemical shifts indicates that only one signal could be observed. The stereospecific assignments that could be established are indicated by underlining. In this case the first chemical shift refers to pro-R proton or group

Residue	Chemical shift δ (p.p.m.)			
	NH	αH	βH	Others
Met-0		4.18	2.19	γCH_2 2.61; εCH_3 2.08;
Arg-1	8.83	4.42	1.85, 1.81	γCH_2 1.68; δCH_2 3.24; εNH 7.23
Arg-2	8.60	4.34	1.82, 1.78	γCH_2 1.67; δCH_2 3.23; εNH 7.23
Lys-3	8.53	4.32	1.81, 1.72	γCH_2 1.48; δCH_2 1.75; εCH_2 3.02; ζNH_3^+ 7.59
Arg-4	8.48	4.32	1.79, 1.72	γCH_2 1.66; δCH_2 3.23; εNH 7.23
Arg-5	8.53	4.36	1.81, 1.66	γCH_2 1.58; δCH_2 3.20; εNH 7.21
Val-6	8.39	4.06	2.00	$\underline{\gamma CH_3\ 0.96, 0.88}$
Leu-7	8.40	4.36	1.51	γCH 1.49; δCH_3 0.91, 0.82
Phe-8	8.13	5.09	$\underline{2.92, 3.35}$	δCH 7.11; εCH 7.33; ζCH 7.50
Ser-9	9.39	4.58	$\underline{4.44, 4.02}$	
Gln-10	9.09	4.05	$\underline{2.10, 2.17}$	γCH_2 2.49, 2.42; εNH_2 7.58, 7.02
Ala-11	8.47	4.22	1.45	
Gln-12	7.77	3.78	2.65, 2.58	γCH_2 1.45; εNH_2 7.32, 6.99
Val-13	8.41	3.20	2.09	$\underline{\gamma CH_3\ 1.06, 1.16}$
Tyr-14	8.45	4.20	$\underline{3.24, 3.10}$	δCH 7.13, εCH 6.81
Glu-15	7.49	4.08	$\underline{1.99, 1.92}$	γCH_2 2.58, 2.29
Leu-16	8.03	3.47	$\underline{0.65, -1.16}$	γCH 1.11; δCH_3 0.47, −0.53
Glu-17	8.52	3.91	$\underline{2.07, 1.95}$	γCH_2 2.61, 2.32
Arg-18	8.08	3.90	$\underline{1.75, 1.62}$	γCH_2 1.56, 1.45; δCH_2 3.11, 2.97; εNH 7.48
Arg-19	7.96	4.28	$\underline{2.23, 2.06}$	γCH_2 1.86; δCH_2 3.54, 3.39; εNH 7.72
Phe-20	8.88	4.70	$\underline{3.05, 3.03}$	δCH 7.05; εCH 7.34; ζCH 6.99
Lys-21	7.80	3.90	1.96	γCH_2 1.55; δCH_2 1.75; εCH_2 3.03; ζNH_3^+ 7.59
Gln-22	7.32	4.29	2.29	γCH_2 2.56, 2.44; εNH_2 7.53, 6.85
Gln-23	8.62	4.48	2.07, 1.97	γCH_2 2.33; εNH_2 7.85, 7.64
Lys-24	8.21	3.91	1.65, 1.43	γCH_2 0.90; δCH_2 1.20, 1.03; εCH_2 2.80, 2.70
Tyr-25	7.56	4.74	$\underline{2.75, 2.96}$	δCH 7.16; εCH 6.81
Leu-26	8.65	4.64	$\underline{1.46, 1.30}$	γCH 0.84; δCH_3 0.46, 0.10
Ser-27	8.97	4.58	4.25, 4.03	
Ala-28	9.28	4.22	1.57	
Pro-29		4.37	2.35, 1.80	γCH_2 2.12, 2.02; δCH_2 3.90, 3.81
Glu-30	7.26	4.07	2.38, 1.86	γCH_2 2.23
Arg-31	8.86	3.77	1.95, 1.86	γCH_2 1.59, 1.30; δCH_2 3.15; εNH 7.25
Glu-32	8.47	3.85	2.16	γCH_2 2.46
His-33	8.15	4.47	$\underline{3.33, 3.30}$	δ^2CH 7.39; ε^1CH 8.63
Leu-34	8.17	4.12	$\underline{1.82, 1.53}$	γCH 1.40; δCH_3 0.96, 0.87
Ala-35	8.49	3.50	1.34	
Ser-36	7.79	4.23	$\underline{3.99, 4.02}$	
Met-37	7.72	4.12	2.35, 2.15	γCH_2 2.51; εCH_3 1.99
Ile-38	7.55	4.49	2.19	γCH_2 1.54, 1.04; γCH_3 0.81; δCH_3 0.55
His-39	7.79	4.39	$\underline{3.58, 3.35}$	δ^2CH 7.23; ε^1CH 8.62
Leu-40	8.13	4.96	$\underline{1.64, 1.05}$	γCH 1.35; δCH_3 0.70, 0.23
Thr-41	8.91	4.92	4.81	γCH_3 1.32
Pro-42		4.09	2.40	γCH_2 2.21, 2.12; δCH_2 3.93
Thr-43	8.01	3.96	4.13	γCH_3 1.33
Gln-44	8.09	4.12	2.69, 2.00	CH_2 2.69, 2.64; εNH_2 7.85, 6.96
Val-45	7.79	3.63	2.23	$\underline{\gamma CH_3\ 0.91, 0.89}$
Lys-46	8.56	4.29	2.33, 1.84	γCH_2 1.57, 1.47; δCH_2 1.56; εCH_2 3.51, 3.26; ζNH_3^+ 7.71
Ile-47	8.73	3.86	2.11	γCH_2 1.82, 1.34; γCH_3 1.04; δCH_3 0.90
Trp-48	8.41	4.29	$\underline{3.43, 3.63}$	δ^1CH 6.98; ε^1NH 10.07; ε^3CH 6.92; ζ^2CH 6.75; ζ^3CH 5.53; η^2CH 5.77
Phe-49	9.29	3.89	$\underline{3.74, 3.36}$	δCH 7.79; εCH 7.53; ζCH 7.10
Gln-50	8.46	3.97	2.31, 2.24	γCH_2 2.50, 2.44; εNH_2 7.78, 6.61
Asn-51	8.77	4.46	$\underline{2.56, 2.84}$	δNH_2 7.63, 6.97
His-52	8.12	3.60	$\underline{1.76, 1.44}$	δ^2CH 5.55; ε^1CH 7.92
Arg-53	8.32	4.22	1.81, 1.74	γCH_2 1.59; δCH_2 3.11; εNH 7.25
Tyr-54	7.84	4.35	$\underline{3.19, 3.12}$	δCH 7.15; εCH 6.85
Lys-55	7.75	3.95	$\underline{1.63, 1.68}$	γCH_2 1.28; δCH_2 1.43; εCH_2 2.84, 2.32; ζNH_3^+ 7.62
Met-56	7.67	4.30	2.19, 2.12	γCH_2 2.69, 2.53; εCH_3 2.13
Lys-57	7.93	4.24	2.22, 1.85	γCH_2 1.44; δCH_2 1.71; εCH_2 3.03; ζNH_3^+ 7.59
Arg-58	8.13	4.22	1.84, 1.72	γCH_2 1.57; δCH_2 3.13; εNH 7.25
Gln-59	8.30	4.28	2.13, 2.03	γCH_2 2.42; εNH_2 7.61, 6.89

Table I (*Continued.*)

Residue	Chemical shift δ (p.p.m.)			
	NH	αH	βH	Others
Ala-60	8.24	4.28	1.44	
Lys-61	8.27	4.25	1.86, 1.82	γCH_2 1.43; δCH_2 1.70; εCH_2 3.02; ζNH_3^+ 7.59
Asp-62	8.30	4.57	2.74, 2.67	
Lys-63	8.25	4.24	1.86, 1.80	γCH_2 1.45; δCH_2 1.70; εCH_2 3.02; ζNH_3^+ 7.59
Ala-64	8.16	4.29	1.43	
Ala-65	8.27	4.28	1.41	
Gln-66	8.31	4.32	2.15, 2.03	γCH_2 2.42; εNH_2 7.61, 6.92
Gln-67	8.09	4.16	2.15, 1.97	γCH_2 2.33; εNH_2 7.57, 6.99

the helices junction of the HTH motif occurring in many DNA-binding proteins [12].

The N-terminal and C-terminal nonapeptides of TTF-1 HD appear devoid of a regular secondary structure. Structural flexibility reaches its maximum in these regions, as do the corresponding DQF COSY and TOCSY intensities of NH-αCH connectivities. This feature emerges also from the H–D exchange rank observed at the same locations (Fig. 2). For most of the terminal residues, in fact, very weakened amide connectivities are still observable, even after 11.5 h average exchange, but with a deceptively high residual intensity in comparison to the detectability threshold of the inherently weaker correlations that arise from poorly flexible residues.

Along with secondary structure information, the analysis of NOESY data also provides with evidence concerning the tertiary organization of TTF-1 HD. The helix segments are observed to occurr at the same locations as in other known HD structures. This conserved spatial arrangement involves contacts between the final residues of helix I and the starting ones of helix II, and between helix I and the virtual junction of helix III rigid and mobile moieties. The last class of contacts forms the central core of the HD structure, with a hydrophobic cluster that includes Phe-20, Trp-48, Phe-49 and His-52.

Quantitative refinement of TTF-1 HD spectral data is still in progress, but the experimental restraints are already sufficient to define a structure that in the region 10–56 displays less than 1.5 Å r.m.s. deviation from the model we predicted earlier [15]. In the same region the internal r.m.s. deviation within the best 10 structures is 1.0 Å, enough to reliably define the backbone topology.

An important feature of that model was the unusual conformation of Tyr-54 side chain [15]. Of the two most commonly adopted (χ^1, χ^2) combinations, i.e. (−73°, 102°) and (180°, 77°) [28], only the latter allowed a satisfactory contact with DNA to be established. Protein data bank conformational frequencies for tyrosines at C-end of α-helices are, however, by far higher for g^+ ($\chi^1 = -60°$) rotamers (70% of occurences) [28].

The experimental observations, based on the analysis of the intervening coupling constants and NOE intensities, point to a clearly biased (61%) conformational distribution around $\chi^1_{54} = 180°$.

Such a degree of experimental validation of our model for the isolated HD increases the reliability of the prediction result obtained for the complex [15].

Here the contacts of the recognition helix (helix III) in the DNA major groove, and those of the N-terminal residues, wrapping the minor groove, should impose a defined geometry to flexible regions of homeodomains.

The flexibility of helix III C-terminal extension and of the N-terminal arginine-rich arm could be responsible for accommodating the interactions with different DNA sequences in TTF-1 HD, as well as in all isolated homeodomains, but it could be largely lost in the entire HD-containing protein. One could speculate that some residual HD mobility might prove functionally advantageous for tuning the interaction specificity, especially in view of the strict steric requirements for successfull HD-DNA binding. Studies are in progress to address these issues.

Acknowledgements: We are indebted with Drs. P. Güntert and G. Vriend who kindly provided the programs DIANA and WHATIF. This work was supported by the Consiglio Nazionale delle Ricerche (CNR), Progetto Finalizzato Ingegneria Genetica.

REFERENCES

[1] Civitareale, D., Lonigro, R., Sinclair, A.J. and Di Lauro, R. (1989) EMBO J. 8, 2537–2542.
[2] Guazzi, S., Price, M., De Felice, M., Damante, G., Mattei, M.G. and Di Lauro, R. (1990) EMBO J. 9, 3631–3639.
[3] Gehring, W.J. (1987) Science 236, 1245–1252.
[4] Scott, M.P., Tamkun, J.W. and Hartzell III, G.V. (1989) Biochim. Biophys. Acta 989, 25–48.
[5] Otting, G., Qian, Y., Billeter, M., Muller, M., Affolter, M., Gehring, W.J. and Wüthrich, K. (1990) EMBO J. 9, 3085–3092.
[6] Kissinger, C.R., Liu, B., Martin-Blanco, E., Kornberg, T. B. and Pabo, C.A. (1990) Cell 63, 579–590.
[7] Wolberger, C., Vershon, A.K., Liu, B., Johnson, A.D. and Pabo, C.A. (1991) Cell 67, 517–528.
[8] Billeter, M., Qian, Y., Otting, G., Müller, M., Gehring, W.J. and Wüthrich, K. (1990) J. Mol. Biol. 214, 183–197.
[9] Otting, G., Qian, Y., Müller, M., Affolter, M., Gehring, W.J. and Wüthrich, K. (1988) EMBO J. 7, 4305–4309.
[10] Phillips C.L., Vershon, A.K., Johnson, A.D. and Dalquist, F.W., Genes Dev. 5, 764–772.

[11] Morita E.M., Shirakawa, M., Hayashi, F., Imagawa, M. and Kyogoku, Y. (1993) FEBS Lett. 321, 107–110.
[12] Pabo, C.A. and Sauer, R.T. (1992) Annu. Rev. Biochem. 61, 1053–1095.
[13] Treisman, J., Harris, E., Wilson, D. and Desplan, C. (1992) Bioassays 14, 145–150.
[14] Damante, G. and Di Lauro, R. (1991) Proc. Nat. Acad. Sci. USA 88, 5388–5392.
[15] Fogolari, F., Esposito, G., Viglino, P., Damante, G. and Pastore, A. (1993) Protein Engineer. 6, 513–519.
[16] Studier, F.W. and Moffat, B.A. (1986) J. Mol. Biol. 189, 113–130.
[17] Müller, M., Affolter, M., Leupin, W., Otting, G., Wüthrich, K. and Gehring, W.J. (1988) EMBO J. 7, 4299–4304.
[18] Braunschweiler, L. and Ernst, R.R. (1983) J. Magn. Reson. 53, 521–528.
[19] Piantini, U., Sorensen, O.W. and Ernst, R.R. (1982) J. Am. Chem. Soc. 104, 6800–6801.
[20] Jeener, J., Meier, B.H., Bachmann, P. and Ernst, R.R. (1979) J. Chem. Phys. 71, 4546–4553.
[21] Drobny, G., Pines, A., Sinton, S., Weitekamp, D. and Wemmer, D. (1979) Faraday Div. Chem. Soc. Symp. 13, 49–58.
[22] Dayringer, H.E., Tramontano, A., Sprang, S.R. and Flatterick, R.J. (1986) J. Mol. Graph. 6, 82–87.
[23] Vriend, G. (1990) J. Mol. Graph. 8, 52–56.
[24] Güntert, P., Braun, W. and Wüthrich, K. (1991) J. Mol. Biol. 217, 517–530.
[25] Wüthrich, K. (1986) NMR of Proteins and Nucleic Acids, Wiley, New York.
[26] Eglander, W.S. and Wand, A.J. (1987) Biochemistry 26, 5953–5958.
[27] Bell, A., Becktel, W.J., Sauer, U., Baase, W.A. and Matthews, B. (1992) Biochemistry 31, 3590–3596.
[28] McGregor, M.J., Islam, S.A. and Sternberg, M.J.E. (1987) J. Mol. Biol. 198, 295–310.